Supporting Information (Uchigashima et al.)

*Animals***.** All animal experiments were performed according to the guidelines for the care and use of laboratory animals of Hokkaido University. The dorsolateral portion of the striatum in adult male C57BL/6N, NL2-knockout (KO) (Jackson Laboratory), CAST-KO (43), D_1R-KO (44), and D_2R-KO (45) mice (1–3 month of age) was analyzed. D_1R-KO and D_2R-KO mice were homozygous for a knock-in mutation in which the human interleukin-2 receptor α-subunit gene was inserted into the D_1R and D_2R genes, respectively. Wild-type and KO littermates were analyzed for comparison. Each of qualitative and quantitative data was obtained from three mice in each animal group.

Fixation. Under deep pentobarbital anesthesia (100 mg/kg of body weight, i.p.), mice were perfused transcardially with 60-75 ml of 4% paraformaldehyde in 0.1 M phosphate buffer (PB, pH 7.2) for 10 min, unless otherwise noted. Striatal tissues perfused with 4% paraformaldehyde/0.1% glutaraldehyde in PB or 2% paraformaldehyde/0.2% picric acid in PB were also used to detect GABA or dopamine receptors, respectively, by post-embedding immunoelectron microscopy.

Section preparation For conventional immunofluorescence and pre-embedding immunoelectron microscopy, sections (20 or 50 μm in thickness) were prepared on a microslicer (VT1000S; Leica) and processed for free-floating incubations. Ultrathin sections (100 nm) were prepared using an ultracryomicrotome (EM-FCS; Leica) after cryoprotection with 0.32M sucrose in PB, and mounted on silane-coated glass slides. For postembedding immunogold electron microscopy, microslicer sections (300 μm) were cryoprotected with 30% glycerol in PB and frozen rapidly with liquid

propane in the EM CPC unit (Leica). Frozen sections were immersed in 0.5% uranyl acetate in methanol at −90°C in the AFS freeze-substitution unit (Leica), infiltrated at −45°C with Lowicryl HM20 resin (Electron microscopy sciences), and polymerized with ultraviolet irradiation. Ultrathin sections were cut with an ultramicrotome (Ultracut; Leica) and mounted on formvar-coated nickel mesh grids. For fluorescent *in situ* hybridization, brains were removed from the skull under deep pentobarbital anesthesia and frozen immediately in powdered dry ice. Fresh frozen sections (20 μm) were cut with a cryostat (CM1900; Leica).

Fluorescent in situ hybridization. We used the following fluorescein- or digoxigenin (DIG)-labeled riboprobes: mouse D_1R (1-950, NM_010076), mouse D_2R (416-1105, NM_010077), and mouse dopamine- and cAMP-regulated neuronal phosphoprotein or protein phosphatase DARPP32 (298-1000; NM_144828). Riboprobe synthesis and *in situ* hybridization were performed following the protocol described previously (36). Nuclear counterstaining was performed using TOTO-3 (Life Technologies). Images were captured using a confocal laser-scanning microscope equipped with a HeNe/Ar laser, and UPLSAPO 10×/0.40 and 20×/0.75 objective lenses (FV1000; Olympus). The specificity of hybridization signals was confirmed by a lack of any significant labeling using the sense riboprobes.

Antibody. Information on the antigens, host species, sources, specificity, and source or references of primary antibodies is summarized in Fig. S7 and Table S1. Briefly, overall patterns of immunofluorescence labeling in coronal striatal sections are provided for tyrosine hydroxylase (TH, Fig. 1A), plasmalemmal dopamine transporter (DAT, Fig. 1B), vesicular monoamine transporter-2 (VMAT2, Fig. S7A), glutamic acid decarboxylase (GAD65/67, Fig. S7B), and vesicular inhibitory amino acid transporter

(VIAAT, Fig. S7C). The specificity of main primary antibodies is shown for cytomatrix protein at the active zone CAST by blank labelings by immunoblot and immunohistochemistry in CAST-KO mice (Fig. 1H, Fig. S7D–S7F); neurexins (Nrxns) by detection of >150 kDa protein bands in the brain and HEK293T cell lysates transfected with Nrxn1α–3α (Fig. S7G and S7H); D_1R and D_2R by the lack of immunolabeling in D_1R-KO and D_2R-KO mice (Fig. S7I–S7L); DARPP32 by selective detection of 32 kDa protein band in the brain and HEK293T cell lysates transfected with DARPP32, similar patterns of DARPP32 immunohistochemistry and *in situ* hybridization, and lack of DARPP32 immunolabeling in striatal interneurons (Fig. S7M-S7Q); gepherin by extensive overlap with NL2 clusters in the striatum and vice versa (Fig. S7S); NL3 by overlap with NL2 clusters (yellow arrows) and wider distribution than NL2 (white arrows) in the striatum (Fig. S7T).

Immunoblot. Whole brains were homogenized using a Potter homogenizer with 15 strokes at 1000 rpm in 10 volumes of ice-cold homogenizing buffer containing 0.32 M sucrose, 1 mM EDTA, 1 mM EGTA, 10 mM Tris-HCl (pH 7.2), and 0.4 mM phenylmethylsulfonyl fluoride. Homogenized samples were centrifuged at 1000 × g for 10 min to remove nuclear fractions. To prepare lysates of transfected cells, HEK293T cells (2×10^6) were transfected with mammalian expression vectors using the calcium phosphate precipitation method, harvested 24–48 h after transfection, and sonicated in 10 volumes of ice-cold homogenizing buffer. Mammalian expression plasmid vectors pCAG-HA-Nrxn1α, pCAG-HA-Nrxn2α, and pCAG-HA-Nrxn3α were kind gifts from Dr. Kensuke Futai (University of Massachusetts Medical School). NL1–4, $GABA_A$Rα1, and DARPP32 cDNAs were amplified from a mouse cDNA library by PCR, subcloned into pTracer-GFP (Life Technologies), and sequenced. The lysates were denatured in 50

mM (±)-dithiothreitol at 65°C for 30 min. Proteins were separated by SDS-PAGE and electroblotted onto transfer membranes (Immobilon-P; Millipore). Membranes were successively incubated with 5% skimmed milk for 30 min, primary antibody (1 μg/ml) for 1 h, and peroxidase-linked secondary antibody (1:10000; Jackson ImmunoResearch) for 1 h. Tris-buffered saline (pH 7.5) containing 0.1% Tween 20 was used as a diluent and washing buffer. Proteins were visualized with ECL prime western blotting detection reagent (GE healthcare).

Immunofluorescence. All incubations were performed at room temperature. Sections were incubated successively with 10% normal donkey serum for 20 min, a mixture of primary antibodies overnight (1 μg/ml), and a mixture of species-specific secondary antibodies for 2 h at a dilution of 1:200 (Life Technologies; Jackson ImmunoResearch; Abcam; Biotium). Combinations of primary and secondary antibodies for multiple immunofluorescence are listed in Table S2. For the detection of $GABA_AR\alpha1$, microslicer sections were subjected to antigen exposure pretreatment before normal donkey serum blocking: 1 mg/ml pepsin in 0.2N HCl at 37°C for 30–60 sec. Phosphate buffer saline (PBS) containing 0.1% Tween 20 was used as a dilution and washing buffer. Images were taken with a confocal laser-scanning microscope equipped with 405-, 473-, 559-, and 647-nm diode laser lines and UPLSAPO 10× (NA, 0.4), PLAPON 60×OSC2 (NA, 1.4; oil immersion), and UPLSAPO 100×S (NA, 1.35; silicone oil immersion) objective lenses (FV1200, Olympus) under the following microscopic settings: zoom factor, 1, 4, 6, and 10; image size, 640×640 pixels; pinhole size, 1 airy unit. Fig. S1H and S2G–S2I were taken with an FV-OSR software module (Olympus) to obtain super-resolution images. To obtain high resolution images shown in Fig. 1A, 1B, S4A, and S7A-S7C, series of images were taken with a UPLSAPO 10×

objective lens (zoom facter 1.3, 256 × 256 pixels) were stitched using FV10-ASW 3.0 (Olympus).

Quantitative assessment of dopamine and GABAergic synapses on GFP-labeled dendrites. To assess the density and molecular expression of dopamine and GABAergic synapses on dendrites of given neuronal types, we labeled single neurons with green fluorescent protein (GFP) by injecting lentiviral vector to the striatum of mice at 4 weeks of age under chloral hydrate anesthesia (350 mg/kg/body weight, i.p.). The lentiviral vector system with murine stem cell virus promoter (MSCV) was kindly provided by St. Jude Children's Research Hospital. The original lentivector pCL20c-MSCV-GFP was modified by adding the woodchuck hepatitis post-transcriptional regulatory element (WPRE) sequence downstream of GFP to enhance GFP expression. Injected mice were fixed 1–2 months later by transcardial perfusion of fixative and processed for multiple immunofluorescence.

We randomly selected GFP-labeled dendrites that ran near and parallel to the section surface, and obtained their z-stacked image series consisting of 20-50 optical sections in steps of 0.2 μm with PLAPON 60×OSC2 and a zoom factor of 6 or 10 for 3D-reconstruction with Imaris (Bitplane) or ImageJ (imagej.nih.gov) software. Dopamine and GABAergic synapses were defined as NL2- or gephyrin-positive clusters on GFP-labeled dendrites in contact with TH-labeled dopaminergic terminals or VIAAT-labeled GABAergic terminals, respectively. Apposition of the three fluorescences was confirmed by images of the X–Y, X–Z, and Y–Z planes. For quantification, we sampled 5–10 dendrites (>10 μm in length and 0.75–1.5 μm in diameter) from each of three mice in each group. The mean length (μm) and the mean diameter (μm) of analyzed dendrites (mean ± SEM) were as follows: 17.7 ± 1.4/1.08 ±

0.03 for d-MSNs (Fig. 4B), 18.0 ± 1.4 and 1.13 ± 0.04 for i-MSNs (Fig. 4C), 17.5 ± 0.87 and 1.09 ± 0.06 for PV-positive interneurons (Fig. S4C), 18.9 ± 2.1 and 0.98 ± 0.04 for nNOS-positive interneurons (Fig. S4D), 15.1 ± 2.0 and 1.10 ± 0.06 for CHT-positive interneurons (Fig. S4E), 20.1 ± 1.2 and 1.04 ± 0.03 for control neurons (Fig. 6A, S6D, S6J), 17.5 ± 2.8 and 0.96 ± 0.03 for NL2-KD#1 neurons (Fig. 6B, S6E, S6K), and 21.8 ± 2.8 and 1.02 ± 0.03 for NL2-KD#2 neurons (Fig. 6C, S6F, S6L). Dendritic spines were also sampled from 6 spiny dendrites from each of three mice. The mean length (μm) of dendritic spines was 1.45 ± 0.03 for d-MSNs and 1.52 ± 0.03 for i-MSNs (Fig. 4D, filled columns). The density of synapses was shown as mean ± SEM of synapse numbers per 10 μm of dendritic shafts or spines. Fluorescent intensities for gephyrin, NL2, and NL3 clusters on GFP-labeled dendritic shafts (mean ± SEM) were measured from 3-4 dendrites in each of three mice, and the background level, as estimated from those in the nucleus, was subtracted (Fig. S6H, I, M). All the images presented in this study were taken as single optical sections.

Criteria of synapses. Synapses were identified by electron microscopy as interneuronal junctions with the following specializations: rigid and parallel apposition of the apposed membranes, the extracellular space stuffed with some electron-dense materials, accumulation of synaptic vesicles and fuzzy active zone in presynaptic elements, and attachment of the postsynaptic density (PSD) to the cytoplasmic side of the postsynaptic membrane. Asymmetric synapses were defined as synapses whose postsynaptic membrane is attached by thick PSD, by which the postsynaptic specialization appeared more dense than the presynaptic specialization (1). In comparison, symmetrical synapses were defined as those having pale and thin PSD, with almost comparable thickness between the postsynaptic and presynaptic

specializations.

By post-embedding immunogold electron microscopy, we identified dopamine synapses as TH-labeled symmetric synapses, GABAergic synapses as VIAAT-labeled symmetrical synapses, and glutamatergic synapses as asymmetrical synapses without TH or VIAAT labeling. To minimize the sampling of false-positive dopamine and GABAergic synapses, we only analyzed symmetric synapses having 5 or more metal particles for TH or VIAAT, respectively, on the presynaptic cytoplasm excluding the mitochondria. The mean and SEM of data obtained from postembedding immunogold analysis were calculated from the mean values of three mice in each group, as shown in Table S3.

Pre-embedding immunoelectron microscopy. For single-label pre-embedding immunogold electron microscopy for D_1R (Fig. 2A), D_2R (Fig. 2B), DAT (Fig. S5G, H), and VMAT2 (Fig. S5K, L), microslicer sections were dipped in Blocking Solutions (Aurion) for 30 min, and incubated overnight with primary antibodies to D_1R (guinea pig), D_2R (rabbit), DAT (rabbit), and VMAT2 (rabbit) (1 μg/ml) diluted with 1% BSA/0.004% saponin in PBS and then with secondary antibodies linked to 1.4-nm gold particles (1:100, Nanogold; Nanoprobes) for 2 h. After postfixaion with 1% glutaraldehyde in PBS for 15 min, immunogold was intensified with a silver enhancement kit (R-GENT SE-EM; Aurion) for 30-60 min.

For double-label pre-embedding immunoelectron microscopy (Fig. 2D, E), sections labeled for guinea pig D_1R or D_2R antibody (metal particles) were further incubated for TH labeling. After blocking with 10% normal guinea pig serum for 30 min, sections were incubated for rabbit TH antibody (1 μg/ml) overnight, biotin-conjugated donkey anti-rabbit secondary antibody (1:200; Jackson

ImmunoResearch) for 2 hr, and peroxidase-conjugated streptoavidin (Nichirei) for 30 min. TH labeling was visualized as 3,3'-diaminobenzidine (DAB) precipitates with a DAB substrate kit (SK-4100; Vector). Immunolabeled sections were treated with 1% osmium tetroxide for 15 min, block-stained with 2% uranyl acetate for 20 min, dehydrated with a graded ethanol series and propylene oxide twice for 10 min each, and embedded in Epon 812 (TAAB). Ultrathin sections were prepared with an ultramicrotome (Ultracut; Leica) and mounted on copper mesh grids.

Quantitative measurement for pre-embedding immunoelectron microsocpy. To avoid uneven antibody penetration, electron micrographs were taken within 5 μm (D_1R or D_2R in Fig. 2A, B, D, E; VMAT2 in Fig. S5K, L) or 10 μm (DAT in Fig. S5F, G) from the surface of sections subjected to pre-embedding immunoelectron microsocpy. To quantify metal particle labeling for D_1R or D_2R (Fig.2C), 3×4 montage images (approximately 3.6 μm × 4.8 μm) were randomly taken at a magnification of 20000×. In double-label pre-embedding immunoelectron microscopy for TH and D_1R or D_2R (Fig. 2G), we searched dendrites, whose profiles formed TH-labeled dopamine synapses and had three or more metal particles for D_1R or D_2R, at a magnification of 4000×. Then, 3×3 montage images (approximately 3.6 μm × 3.6 μm) over dopamine synapses were taken at a magnification of 20000×, and 4–7 dopamine synapses were sampled from each of three mice in each group. The density of labeling was calculated per 1 μm of the synaptic, perisynaptic, and extrasynaptic membranes.

Metal particles for VMAT2 were also measured at dopamine synapses as the density per 1 μm^2 of the cytoplasm (Fig. S5M) by sampling nerve terminals, which contained five or more particles for VMAT2 and formed symmetric synapses with dendriteic shafts and spines. We took 3×3 montage images (approximately 3.6 μm × 3.6

μm) at a magnification of 20000×, with 5–8 terminals from each of three mice in each group.

Post-embedding immunoelectron microscopy. Double-label post-embedding immunogold electron microscopy was employed to quantify molecular expression at TH-labeled dopamine synapses (Fig. 1E, 1G, II, 3D-F, S2J, S2K, S3S, S3E, S5P, S5Q, S5U, S5V) or at VIAAT-labeled GABAergic synapses (Fig. 1D, S1I-L, S3A-C). Ultrathin sections on nickel grids were successively treated with the following solutions: saturated sodium ethoxide for 2 sec, 50 mM glycine in incubation solution (0.03% Triton X-100 in Tris-buffered saline, pH 7.4; TBST) for 10 min, blocking solution containing 2% normal goat serum in TBST (GTBST) for 10 min, primary antibodies (1:1000 dilution for GABA antibody and 20 μg/ml for CAST, , D_1R, D_2R, $GABA_A$Rα1, gephyrin, NL2, NL3, Nrxn pan-AMPAR, PSD-95,) diluted in GTBST overnight, and colloidal gold-conjugated (10 nm diameter) secondary antibodies (1:100; British BioCell International) in GTBST for 2 hr. After blocking with 2% normal rabbit or guinea pig serum in TBST, sections were subjected successively to mouse or rabbit TH antibody or rabbit or guinea pig VIAAT antibody in GTBST (20 or 10 μg/ml, respectively) for 6 hr and colloidal gold-conjugated (15 nm diameter) secondary antibodies (1:100; British BioCell International) in GTBST for 2 hr. Sections were washed thoroughly in distilled water, and stained with 5% uranyl acetate in 40% EtOH for 90 sec and Reynold's lead citrate solution for 90 sec. Photographs were taken with a JEM1400 electron microscope (JEOL).

Quantitative measurement for post-embedding immunoelectron microscopy. First we searched asymmetrical synapses or symmetrical synapses with immunogold labeling for TH or VIAAT at a magnification of 5000×, and took 3×3 montage images

(approximately 2.4 μm × 2.4 μm) of glutamatergic, dopamine, and GABAergic synapses at a magnification of 30000×. To measure the density of presynaptic labeling for Nrxn (Fig. 1J, S1) and postsynaptic labeling for $GABA_AR\alpha1$, gephyrin, NL2, NL3, PSD-95, and AMPAR (Fig. 3G-I; Fig. S3F, S3G, S5R, S5W), immunogold particles < 20 nm apart from the center of the cell membrane were measured. In assessment of presynaptic labeling for CAST (Fig. 1H), we counted immunogold particles < 40 nm from the center of the presynaptic membrane. We examined 5–15 dopamine, GABAergic, or glutamatergic synapses from each of three mice in each group, with the number of analyzed synapses ranging < 7 synapses in the same groups. Metal particles for GABA were also measured at dopamine, GABAergic, or glutamatergic synapses as the density per 1 μm^2 of the cytoplasm excluding the mitochondria (Fig. 1F).

The density of D_1R and D_2R labelings on the synaptic, perisynaptic, and extrasynapti membranes at around dopamine synapses (Fig. S2L, M) was calculated by measuring immunogold particles < 20 nm apart from the center of the cell membrane in contact with TH-labeled dopamine terminals. From each of three mice, 17–20 dendritic profiles forming dopamine synapses were analyzed. The density of immunogold labeling at given synapse types or compartments was calculated as that per 1 μm of the synaptic, perisynaptic, and extrasynaptic membranes.

Dopamine synapse density. The density of dopamine synapses in the striatum was compared between NL2-KO and wild-type mice by measuring the nearest neighbor distance (Fig. S5H). Dopamine synapses, which were labeled with five or more metal particles for DAT and formed symmetric synapses on dendritic shafts and spines, were sampled, and their 5×5 montage images (approximately 11 μm × 11 μm) were taken at a magnification of 10000×. We measured distances from the center of the postsynaptic

membrane of given dopamine synapses to that of the nearest ones, and the mean nearest neighbor distance was calculated by sampling 5–8 dopamine synapses from each of three mice in each group.

Knockdown by microRNA. For miR-based knockdown, we used the BLOCK-iT Pol II miR RNAi Expression Vector Kits (Life Technologies) according to the manufacturer's instructions. pCL20c-MSCV-GFP-miR-WPRE was obtained by inserting the following miR sequences into pCL20c-MSCV-GFP-WPRE: 5'-GTGTACATCCTGGTCCACTAGCGTTTTGGCCACTGACTGACGCTAGTGGCAGGATGTACAC-3' (NL2-miR#1); 5'-GTGAACTTGGTGTCCTGTGGCAGTTTTGGCCACTGACTGACTGCCACAGCACCAAGTTCA-3' (NL2-miR#2); 5'-GAAATGTACTGCGCGTGGAGACGTTTTGGCCACTGACTGACGTCTCCACGCAGTACATTT-3' (control-miR).

Lentiviral vectors were produced by co-transfection of HEK293T cells (5×10^6 per 1 dish) with a mixture of pCL20c-MSCV-GFP-WPRE or pCL20c-MSCV-GFP-miR-WPRE (20 μg per 1 dish), pCAG-kGP4.1R (12 μg), pCAG4-RTR2 (4 μg), and pCAGGS-VSVG (4 μg) using the calcium phosphate precipitation method. HEK293T cells were incubated in DMEM (D5796; Sigma) supplemented with 10% fetal bovine serum (Cell Culture Bioscience), 1× penicillin/streptomycin (P4333; Sigma), 1 mM sodium pyruvate (S8636; Sigma), 1× MEM non-essential amino acid solution (M7145; Sigma), and 1× GlutaMAX (#35050061; Life Technologies) at 37°C in a 10% CO_2 atmosphere. Culture medium was replaced with Ultraculture (12-725F, Lonza) 16 hr after transfection. Supernatant containing viral particles was collected 40 h after transfection, centrifuged at 1000 × g

for 10 min, filtered through 0.45 μm membranes, and concentrated using an Amicon Ultra filter unit 100k (Millipore). Viral solution was further concentrated by centrifuging at 6000 × g for 16 hr, before suspending in PBS. Viral titer (expressed as transducing units [TU]) was calculated as $1.0 \times 10^{8–9}$ TU/ml by measuring the number of infected HEK293T cells.

For viral injection in newborn pups, deep anesthesia was obtained by lowering the body temperature on ice, and the skull was fastened with a hand-made stereotaxic instrument. A glass pipette (G-1.2; Narishige) filled with 0.5 μl of viral solution was inserted into the striatum. Viral solutions were injected by air pressure (Pneumatic Picopump; World Precision Instruments). Injected mice were fixed 2 months later by transcardial perfusion of fixative as described above.

Co-culture assay. Co-culture experiments were performed according to previous methods with modifications (32). Briefly, the midbrain and striatum from newborn mice were collected in ice-cold Hank's balanced solution (HBS), and dissociated in 0.25% trypsin/HBS for 10 min and 0.25% trypsin/0.1% DNaseI/HBS for 5 min at 37°C. Dissociated neurons were suspended in neuronal basal medium supplemented with B-27 solution (both from Life Technologies) and GlutaMAX, seeded on plastic dishes coated with 5% Matrigel (BD Biosciences) at a density of $1–3 \times 10^4$ cells/cm^2, and incubated at 5% CO_2. After 9–11 days *in vitro*, HEK293T cells transfected with pTracer-NL1, pTracer-NL2, pTracer-NL3, pTracer-$GABA_AR\alpha1$, and pEGFP-N1 (Clontech) were seeded on the primary midbrain or striatal culture at a density of 2×10^4 cells/cm^2. After 48 hr, cells were fixed with 4% paraformaldehyde in 0.1M PB for 10 min at room temperature for immunofluorescence.

Statistical analysis. For quantitative comparison, immunofluorescence data

from three mice in each group were pooled together and are presented as the mean ± SEM. Statistical significance was assessed by Mann–Whitney U test (for comparison of two independent samples) or one-way ANOVA with Tukey's *post hoc* test (for comparison of more than three independent samples). Statistical significance of quantitative electron microscopic data was assessed by unpaired *t* test, because no significant differences were found in variances between two independent samples by F-test.

SI Figure Legends

Fig. S1 Presynaptic phenotype at striatal dopamine synapses is neither glutamatergic nor GABAergic. (*A–F*) Double immunofluorescence for DAT (green) and terminal markers (red), including VGluT1 (*A*), VGluT2 (*B*), VGluT3 (*C*), GAD (*D*), VIAAT (*E*), or GAT1 (*F*). Ultrathin (100 nm) sections were used to increase the spatial resolution of fluorescent signals. Note the lack of glutamatergic and GABAergic molecular expression in DAT-positive dopaminergic terminals, except for weak immunoreactivity for GAT1 (arrows in *F*). (*G*) Triple immunofluorescence for DAT (green), GAT1 (red), and VIAAT (blue) showing much stronger expression of GAT1 in VIAAT-labeled GABAergic terminals (arrowheads) than in DAT-labeled dopaminergic terminals (arrows). (*H*) Super-resolution immunofluorescence images for CAST (red) and DAT (green). Tiny CAST-positive puncta are detected in some portions of large DAT-positive dopaminergic terminals (arrows). (*I–L*) Double-label post-embedding immunoelectron microscopy for VIAAT (Ø = 15-nm colloidal gold particles) and CAST (*I* and *J*; Ø = 10 nm) or Nrxn (*K* and *L*; Ø = 10 nm). Immunogold labeling for CAST and Nrxn is observed beneath the presynaptic membrane at VIAAT-positive symmetric or GABAergic synapses (NT-GABA; *I* and *K*) and VIAAT-negative asymmetric or glutamatergic synapses (NT-Glu; *J* and *L*). Pairs of open and filled arrowheads indicate the synaptic membrane of symmetric and asymmetric synapses, respectively. Dn, dendrite; Sp, spine. Scale bars: 2 μm (*A–H*), 100 nm (*I–L*).

Fig. S2 Expression of D_1R and D_2R in striatal MSNs. (*A*) Fluorescent *in situ* hybridization for D_1R (red) and D_2R (green) mRNAs and nuclear counterstaining with

TOTO-3 (blue). (*B*) Double immunofluorescence for D_1R (red) and D_2R (green). Cell bodies and neuropils are labeled for D_1R (D1) and D_2R (D2) in a segregated manner. (*C–F*) Quadruple immunofluorescence for D_1R (red), D_2R (green), MAP2 (white), and neuronal markers (blue), including DARPP32 (*C*), PV (*D*), nNOS (*E*), and CHT (*F*). In MAP2-labeled dendrites (arrowheads), DARPP32-positive MSNs express either D_1R or D_2R at high levels (*C*), whereas various interneurons are low or negative in expression of dopamine receptors (*D–F*). (*G*) Triple immunofluorescence for D_1R (red), tau (white), and DARPP32 (blue) showing weak expression of D_1R in tau-labeled axons of DARPP32-positive MSNs (arrowheads). (*H* and *I*) Triple immunofluorescence for D_2R (green), tau (white), and CHT (*H*; blue) or DAT (*I*; blue) showing moderate expression of D_2R in tau-labeled axons of CHT-positive cholinergic (*H*, arrowheads) and DAT-positive dopaminergic axons (*I*, arrowheads). (*J* and *K*) Double-label post-embedding immunoelectron microscopy for TH (Ø = 15-nm colloidal gold particles) and D_1R (*J*, Ø = 10 nm) or D_2R (*K*, Ø = 10 nm) showing predominant extrasynaptic and perisynaptic labeling (arrows) of dendrites (Dn) forming symmetric synapses (open arrowhead pairs) with TH-positive dopaminergic terminals (NT-DA). Tissue specimens were mildly fixed with 0.2% picric acid/2% paraformaldehyde to increase the sensitivity of dopamine receptor detection. (*L and M*) Densities (mean ± SEM; n =3 mice for each) for D_1R (L; 55 synapses) and D_2R (right; 60 synapses) labelings per 1 μm of the synaptic, perisynaptic, and extrasynaptic membranes. The length of the plasma membrane (μm; in parentheses) and the number of metal particles analyzed are indicated above each column. $*p < 0.05$ (unpaired *t* test). Scale bars: 20 μm (*A* and *B*), 2 μm (*C–I*), 100 nm (*J and K*).

Fig. S3 Expression of GABAergic, but not glutamatergic, postsynaptic proteins at dopamine synapses. (*A–C*) Double-label post-embedding immunoelectron microscopy for $GABA_AR\alpha1$ (*A*; Ø = 10-nm colloidal gold particles), gephyrin (*B*; Ø = 10 nm), or NL2 (*C*; Ø = 10 nm), and for VIAAT (Ø = 15 nm). Immunogold particles for $GABA_AR\alpha1$, gephyrin, or NL2 (arrows) are concentrated at symmetric synapses formed by VIAAT-labeled GABAergic terminals (NT-GABA, open arrowhead pairs). (*D* and *E*) Double-label post-embedding immunoelectron microscopy for TH (Ø = 15-nm colloidal gold particles) and PSD-95 (*D*; Ø = 10 nm) or AMPA receptor (AMPAR; *E*; Ø = 10 nm) in the striatum. Immunogold particles for PSD-95 and AMPAR (arrows) are found on the postsynaptic membrane at TH-negative asymmetric synapses on dendritic spines (glutamatergic, filled arrowhead pairs), but not at TH-positive symmetric synapses (dopamine, open arrowhead pairs). Dn, dendrite; NT-DA, dopaminergic nerve terminal; NT-Glu, glutamatergic nerve terminal; Sp, spine. (*F* and *G*) The density (mean ± SEM; 3 mice for each) of immunogold labeling for PSD-95 (*F*) or AMPAR (*G*) per 1 μm of the synaptic membrane at dopamine (DA), GABAergic (GABA), and glutamatergic (Glu) synapses. The numbers of total synapses analyzed are indicated above each column. $*p < 0.05$, $***p < 0.001$ (unpaired *t* test). Scale bars: 100 nm.

Fig. S4 Dopamine synapses are sparse on dendrites of striatal interneurons. (*A* and *B*) Lentiviral GFP labeling of striatal neurons at low (*A*) and high magnifications (*B*, single striatal neuron). Cx, cortex; NA, nucleus accumbens; St, striatum. (*C–E*) Quadruple immunofluorescence for NL2 (red), GFP (green), TH (blue), and interneuron markers (white), including PV (*C*), nNOS (*D*), and CHT (*E*). Note that NL2 clusters on

GFP-labeled interneuron dendrites (white arrowheads) rarely appose TH-positive dopaminergic terminals. Scale bar: 100 μm (*A*), 10 μm (*B*), 2 μm (*C–E*)

Fig. S5 NL2-mediated presynaptic differentiation of GABAergic axons *in vitro* (A-E), NL3-mediated presynaptic differentiation of dopaminergic axons *in vitro* (F), and unaffected dopamine synapse formation and compensatory NL3 upregulation in the striatum of NL2-knockout mice (G-X). (*A*) A schematic illustration of co-culture assay of striatal neurons with HEK293T cells transiently expressing NL2, $GABA_AR\alpha1$, or GFP. Because striatal neurons are exclusively GABAergic, tau-positive axons were discerned as GABAergic axons in this experiment. (*B–D*) Triple immunofluorescence for CAST (red) and DAT (green), and for NL2 (*B*; blue), $GABA_AR\alpha1$ (*C*; blue) or GFP (*D*; blue). CAST clusters are recruited to contact sites (arrowheads) of striatal GABAergic axons with HEK293T cells expressing NL2 (*B*), but not $GABA_AR\alpha1$ (*C*) or GFP (*D*). (*E*) The density of CAST clusters per 100 μm of striatal GABAergic axons in contact with HEK293T cells. The number of HEK293T cells contacted by tau-labeled striatal GABAergic axons analyzed is indicated above each column. ***$p < 0.001$ (one-way ANOVA with Tukey's *post hoc* test). (*F*) Triple immunofluorescence for CAST (red), DAT (green), and NL3 (blue) in co-cultures of midbrain dopamine neurons with HEK293T cells expressing NL3. Note NL3 expressed in HEK293T cells induces CAST clustering at contact sites with DAT-labeled dopaminergic axons (arrowheads). (*G and H*) Pre-embedding immunoelectron microscopy for DAT in wild-type (*G*) and NL2-knockout (KO) (*H*) mice. DAT-positive dopamine synapses in the boxed areas of (*G*) or (*H*) are enlarged in (*G'*) and (*G"*), or (*H'*) and (*H"*), respectively. Open arrowhead pairs indicate symmetric contacts at

DAT-positive dopamine synapses. (*I*) Nearest-neighbor distances (μm) between dopamine synapses in wild-type (open column) and NL2-KO (filled column) mice. (*J–X*) Immunofluorescence and immunogold labeling for VMAT2 (*J–N*), gephyrin (*O–S*), and NL3 (*T–X*) in the striatum of wild-type (*J, L, O, Q, T,* V) and NL2-KO (*K, M, P, T, U, W*) mice. Pre-embedding immunoelectron microscopy was applied for VMAT2 (*L, M*), while double-label post-embedding immunoelectron microscopy was employed for TH (*Ø* = 15-nm colloidal gold particles; *Q, R, V, W*) and gephyrin (*Ø* = 10 nm; *Q, R*) or NL3 (*Ø* = 10 nm; *V, W*). Bar graphs show the densities (mean ± SEM; n =3 mice for each) of VMAT2 labeling (*N*) per 1 μm^2 of dopaminergic terminals and of gephyrin (*S*) or NL3 (*X*) labeling per 1 μm of dopamine synapses in wild-type (open columns) and NL2-KO (filled columns) mice. Note that immunofluorescence intensity of NL3 in wild-type mice is low to moderate (*T*), whereas that in NL2-knockout mice is elevated in some clusters (*U,* arrows). Open arrowhead pairs indicate symmetric contacts at dopamine synapses. Dn, dendrite; NT-DA, dopaminergic nerve terminal. The numbers of total synapses analyzed are indicated above each column (*I, N, S, X*). *$p < 0.05$ (unpaired *t* test). Error bars represent SEM. Scale bars: 2 μm (*B–D,* J, *K, O, P, T,* and *U*), 1 μm (*G* and *H*), 200 nm (*G', G", H'*, and *H"*), 100 nm (*L, M, Q, R, V,* and *W*).

Fig. S6 Lentivirus-mediated sparse knockdown of NL2 in the striatum *in vivo*. (*A*) Immunoblot for NL2-knockdown (KD) efficiency and specificity in HEK293T cells expressing NL1, NL2, and NL3. (*B*) Lentiviral vectors (LV) were injected into the striatum at birth, and analysis was conducted at 2 months of age. (*C*) Double immunofluorescence for GFP and DARPP32 in the adult striatum. Most of GFP-labeled neurons are DARPP32-positive MSNs (arrows). (*D–F* and *J–L*) Triple

immunofluorescence for NL2 (*D–F*; gray) or NL3 (*J–L*; gray), gephyrin (red), and GFP (green) in spiny dendrites of control (*D* and *J*), NL2-KD#1 (*E* and *K*), or NL2-KD#2 (*F* and *L*) neurons. White and yellow arrowheads indicate gephyrin clusters on infected (GFP-labeled) and non-infected (GFP-unlabeled) dendrites, respectively. (*G–I* and *M*) The density of gephyrin clusters per 10 μm of control and KD dendrites (*G*), and fluorescence intensity (arbitrary units) of gephyrin (*H*), NL2 (*I*), and NL3 (*M*) clusters. Total numbers of dendrites (*G*) or gephyrin clusters (*H*, *I*, and *M*) analyzed are indicated above each column. Error bars represent SEM. ***$p < 0.001$ (Mann–Whitney U test). Scale bar: 20 μm (*C*), 2 μm (*D–F* and *J–L*).

Fig. S7 Specificity of primary antibodies used in the present study. (*A–C*) VMAT2, GAD, and VIAAT antibodies. Patterns of immunofluorescence labeling for VMAT2 (*A*), GAD (*B*), and VIAAT (*C*) are shown in coronal sections through the striatum. (*D–F*) CAST antibody. Specific detection of CAST band at 130 kDa in immunoblot *(D*) and specific immunofluorescence labeling of CAST (red) in synaptophysin-labeled nerve terminals (green) (*E* and *F*) are shown in brain tissues from wild-type mice, but not CAST-knockout (KO) mice. (*G* and *H*) Nrxn1α antibody. Owing to high sequence homology in the C terminus of Nrxn1α–3α (*G*), immunoblot detects 120–150-kDa bands in brain homogenates and HEK293T cell lysates transfected with Nrxn1α, 2α, and 3α (*H*). (*I-L*) D_1R and D_2R antibodies. Note the lack of immunofluorescence signals for D_1R and D_2R in brains of D_1R-KO and D_2R-KO mice, respectively. (*M–Q*) DARPP32 antibody. Immunoblot detects 32 kDa band in both brain homogenates and HEK293T cell lysates expressing DARPP32 (*M*). Note similar patterns of labeling by fluorescent *in situ* hybridization for DARPP32 mRNA (*N*) and immunohistochemistry

for DARPP32 (*O*) in parasagittal brain sections. Double immunofluorescence for DARPP32 (*P, Q*, red) and PV (*P*, green) or CHT (*Q*, green) shows the lack of DARPP32 labeling in PV- and CHT-expressing interneurons (asterisks). (*R–T*) NL1, NL2, and NL3 antibodies. Immunoblot with NL1 (top), NL2 (middle) and NL3 (bottom) antibodies selectively detects 100–150-kDa protein bands in brain homogenates and HEK293T cell lysates expressing NL1–4 (*R*). Double immunofluorescence shows that NL2 (green) overlaps well with gephyrin (red) in the striatum (*S*). Triple immunofluorescence for NL2 (green), NL3 (red), and DAT (blue) shows that NL3 is expressed at both NL2+/DAT- synapses (yellow arrows) and NL2+/DAT+ dopamine synapses (white arrows) (*T*). Cb, cerebellum; Cx, cortex; Hi, hippocampus; MO, medulla oblongata; NA, nucleus accumbens; St, striatum; Th, thalamus. Scale bars: 1 mm (*A–C*, *I–L*, *N*, and *O*), 20 μm (*P* and *Q*), 2 μm (*E*, *F*, *S*, *and T*).

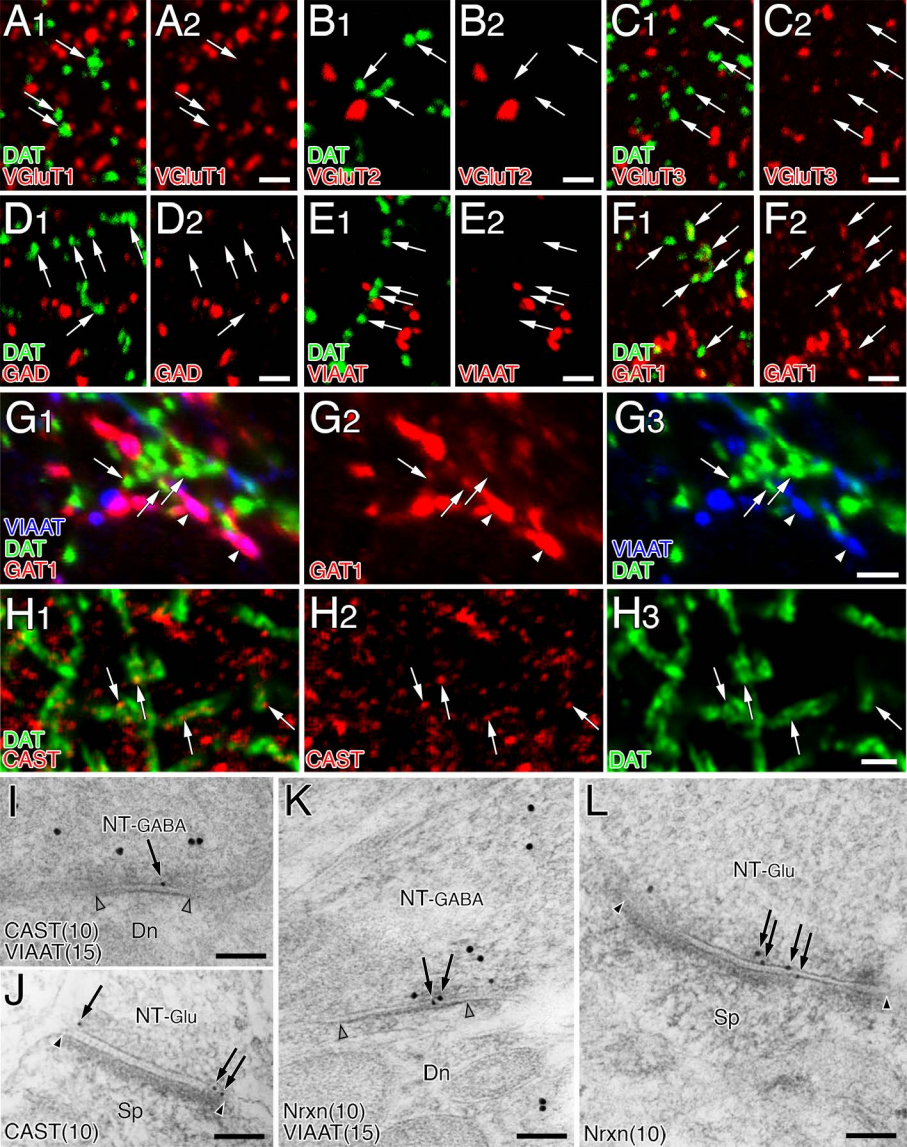
A1
DAT
VGluT1
A2
VGluT1
B1
DAT
VGluT2
B2
VGluT2
C1
DAT
VGluT3
C2
VGluT3
D1
DAT
GAD
D2
GAD
E1
DAT
VIAAT
E2
VIAAT
F1
DAT
GAT1
F2
GAT1
G1
VIAAT
DAT
GAT1
G2
GAT1
G3
VIAAT
DAT
H1
DAT
CAST
H2
CAST
H3
DAT
I
NT-GABA
CAST(10)
VIAAT(15)
Dn
J
NT-Glu
Sp
CAST(10)
K
NT-GABA
Dn
Nrxn(10)
VIAAT(15)
L
NT-Glu
Sp
Nrxn(10)

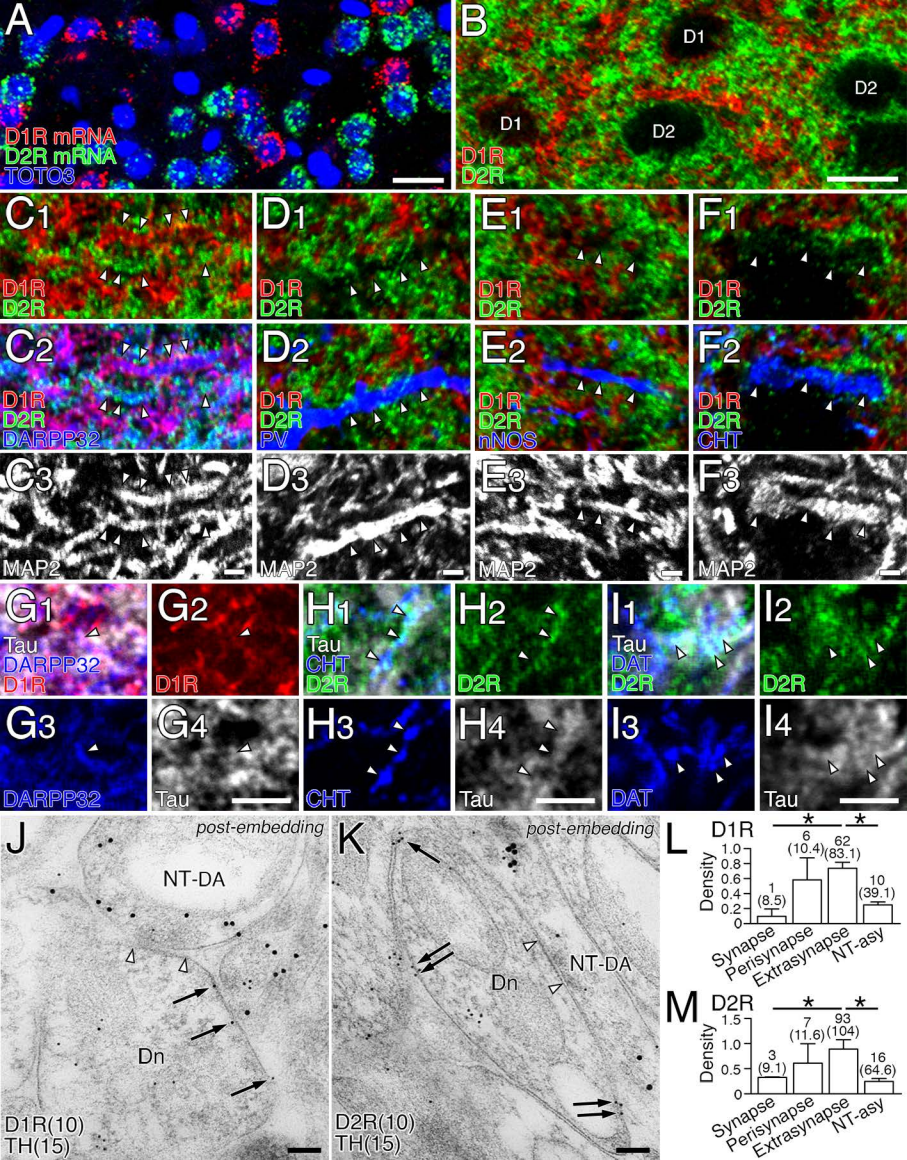
A
D1R mRNA
D2R mRNA
TOTO3
B
D1
D2
D1
D2
D1R
D2R
C1
D1R
D2R
D1
D1R
D2R
E1
D1R
D2R
F1
D1R
D2R
C2
D1R
D2R
DARPP32
D2
D1R
D2R
PV
E2
D1R
D2R
nNOS
F2
D1R
D2R
CHT
C3
MAP2
D3
MAP2
E3
MAP2
F3
MAP2
G1
Tau
DARPP32
D1R
G2
D1R
H1
Tau
CHT
D2R
H2
D2R
I1
Tau
DAT
D2R
I2
D2R
G3
DARPP32
G4
Tau
H3
CHT
H4
Tau
I3
DAT
I4
Tau
J
post-embedding
NT-DA
Dn
D1R(10)
TH(15)
K
post-embedding
NT-DA
Dn
D2R(10)
TH(15)
L
D1R
Density
1.0
0.8
0.6
0.4
0.2
0
1
(8.5)
6
(10.4)
62
(83.1)
10
(39.1)
Synapse
Perisynapse
Extrasynapse
NT-asy
M
D2R
Density
1.5
1.0
0.5
0
3
(9.1)
7
(11.6)
93
(104)
16
(64.6)
Synapse
Perisynapse
Extrasynapse
NT-asy

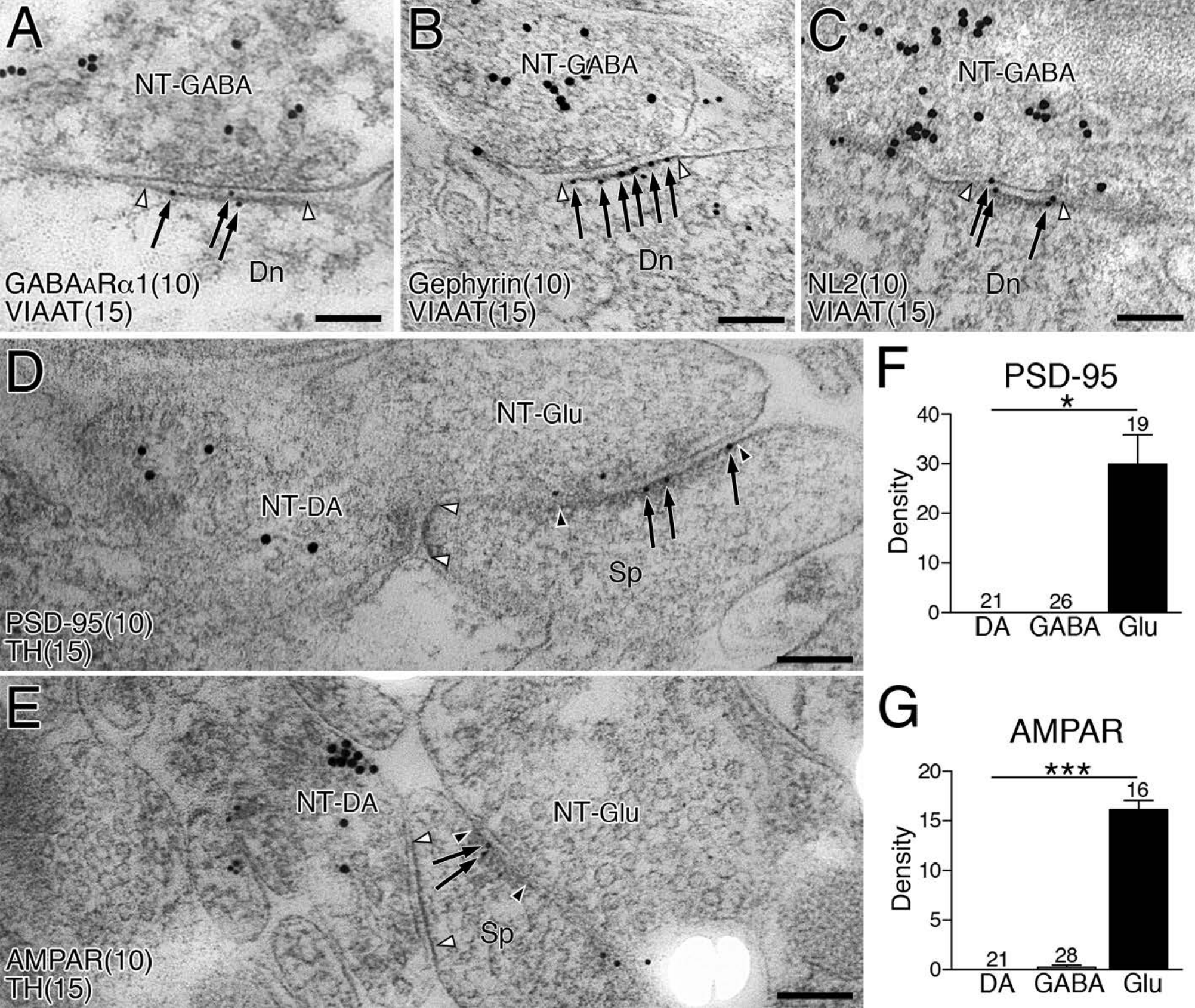
A
NT-GABA
Dn
GABAAR α1(10)
VIAAT(15)
B
NT-GABA
Dn
Gephyrin(10)
VIAAT(15)
C
NT-GABA
Dn
NL2(10)
VIAAT(15)
D
NT-Glu
NT-DA
Sp
PSD-95(10)
TH(15)
E
NT-DA
NT-Glu
Sp
AMPAR(10)
TH(15)
F
PSD-95
*
Density
40
30
20
10
0
19
21
26
DA
GABA
Glu
G
AMPAR
***
Density
20
15
10
5
0
16
21
28
DA
GABA
Glu

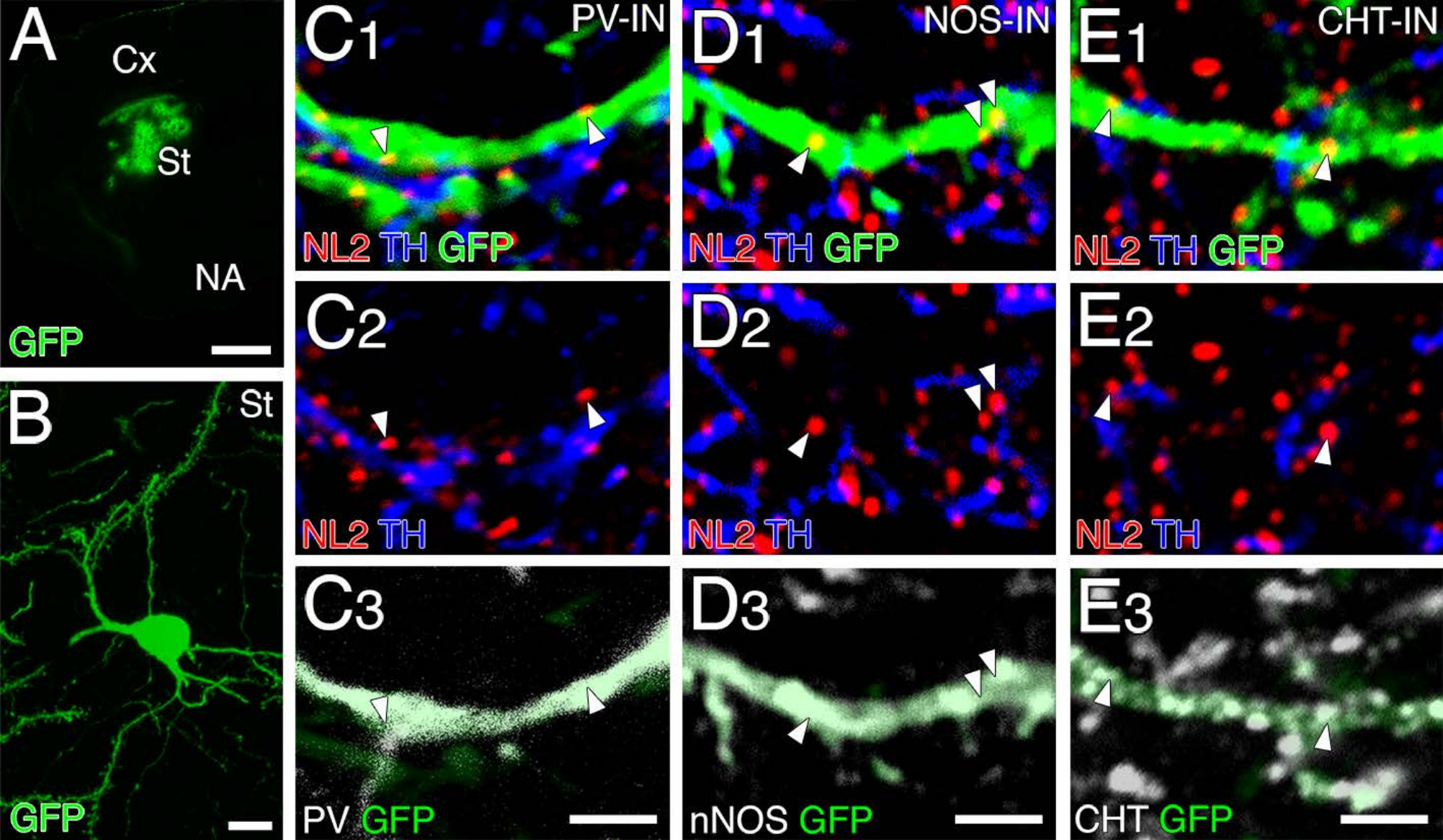
A
Cx
St
NA
GFP
B
St
GFP
C1
PV-IN
NL2 TH GFP
C2
NL2 TH
C3
PV GFP
D1
NOS-IN
NL2 TH GFP
D2
NL2 TH
D3
nNOS GFP
E1
CHT-IN
NL2 TH GFP
E2
NL2 TH
E3
CHT GFP

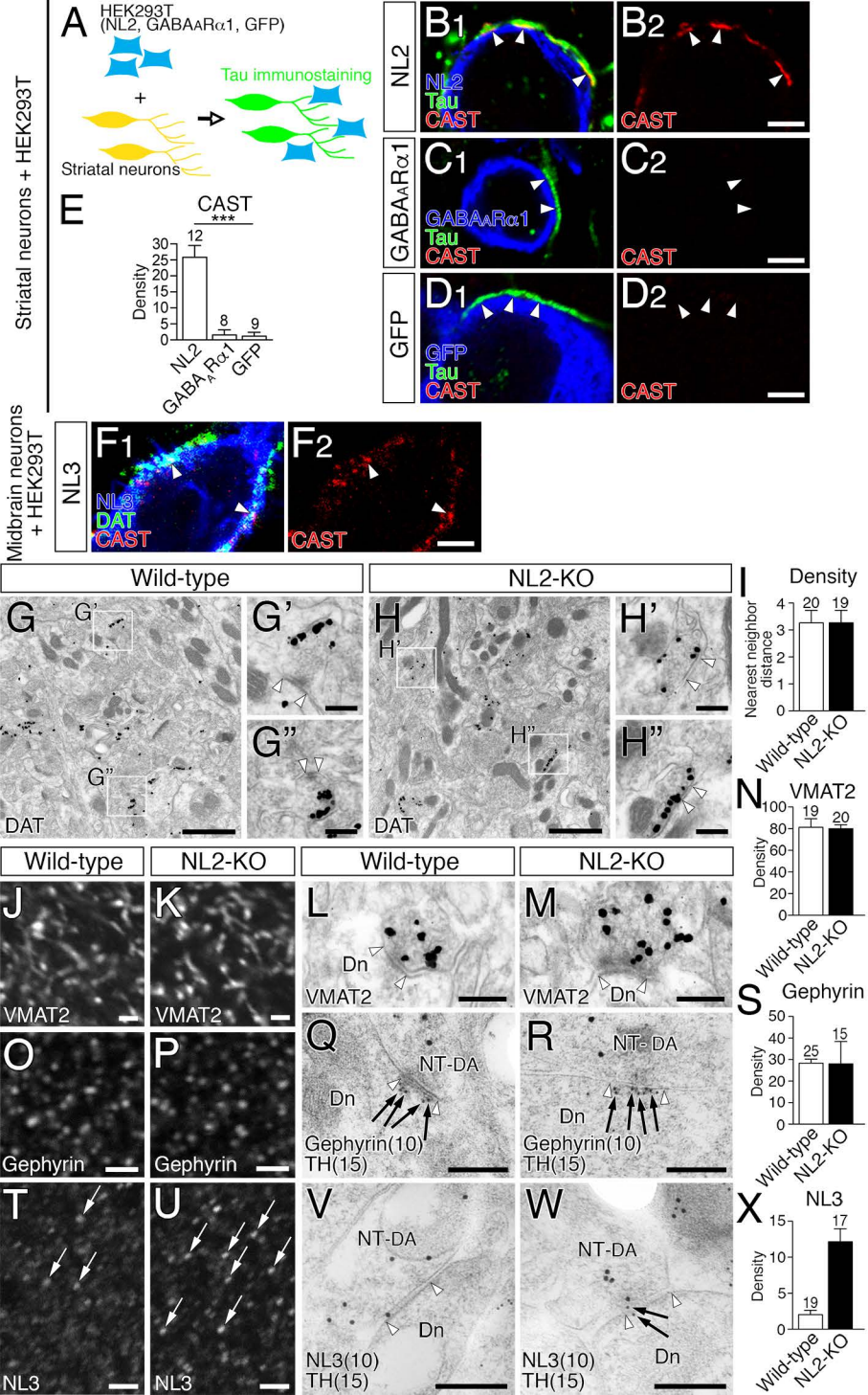
Striatal neurons + HEK293T
A
HEK293T
(NL2, GABAARα1, GFP)
+
Striatal neurons
Tau immunostaining
E
CAST
***
Density
30
25
20
15
10
5
0
12
8
9
NL2
GABAARα1
GFP
NL2
B1
NL2
Tau
CAST
B2
CAST
GABAARα1
C1
GABAARα1
Tau
CAST
C2
CAST
GFP
D1
GFP
Tau
CAST
D2
CAST
Midbrain neurons + HEK293T
NL3
F1
NL3
DAT
CAST
F2
CAST
Wild-type
NL2-KO
G
G'
G''
DAT
H
H'
H''
DAT
I
Density
Nearest neighbor distance
4
3
2
1
0
20
19
Wild-type
NL2-KO
N
VMAT2
Density
100
80
60
40
20
0
19
20
Wild-type
NL2-KO
S
Gephyrin
Density
50
40
30
20
10
0
25
15
Wild-type
NL2-KO
X
NL3
Density
15
10
5
0
19
17
Wild-type
NL2-KO
Wild-type
NL2-KO
Wild-type
NL2-KO
J
VMAT2
K
VMAT2
L
Dn
VMAT2
M
VMAT2
Dn
O
Gephyrin
P
Gephyrin
Q
NT-DA
Dn
Gephyrin(10)
TH(15)
R
NT-DA
Dn
Gephyrin(10)
TH(15)
T
NL3
U
NL3
V
NT-DA
Dn
NL3(10)
TH(15)
W
NT-DA
Dn
NL3(10)
TH(15)

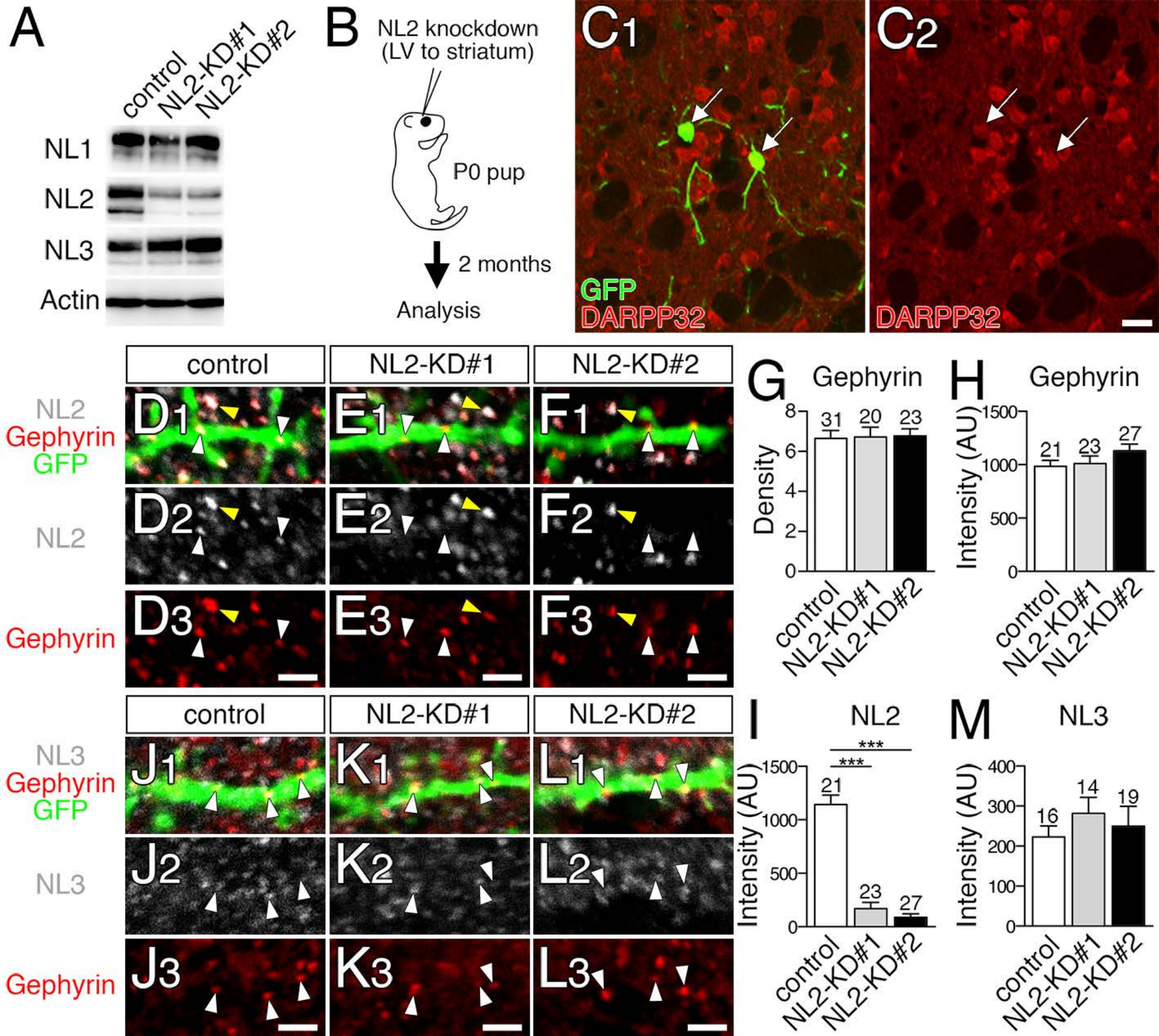
A
control
NL2-KD#1
NL2-KD#2
NL1
NL2
NL3
Actin
B
NL2 knockdown
(LV to striatum)
P0 pup
2 months
Analysis
C1
GFP
DARPP32
C2
DARPP32
control
NL2-KD#1
NL2-KD#2
NL2
Gephyrin
GFP
D1
E1
F1
D2
E2
F2
NL2
D3
E3
F3
Gephyrin
G
Gephyrin
Density
31
20
23
control
NL2-KD#1
NL2-KD#2
H
Gephyrin
Intensity (AU)
21
23
27
control
NL2-KD#1
NL2-KD#2
control
NL2-KD#1
NL2-KD#2
NL3
Gephyrin
GFP
J1
K1
L1
J2
K2
L2
NL3
J3
K3
L3
Gephyrin
I
NL2
***
***
Intensity (AU)
21
23
27
control
NL2-KD#1
NL2-KD#2
M
NL3
Intensity (AU)
16
14
19
control
NL2-KD#1
NL2-KD#2

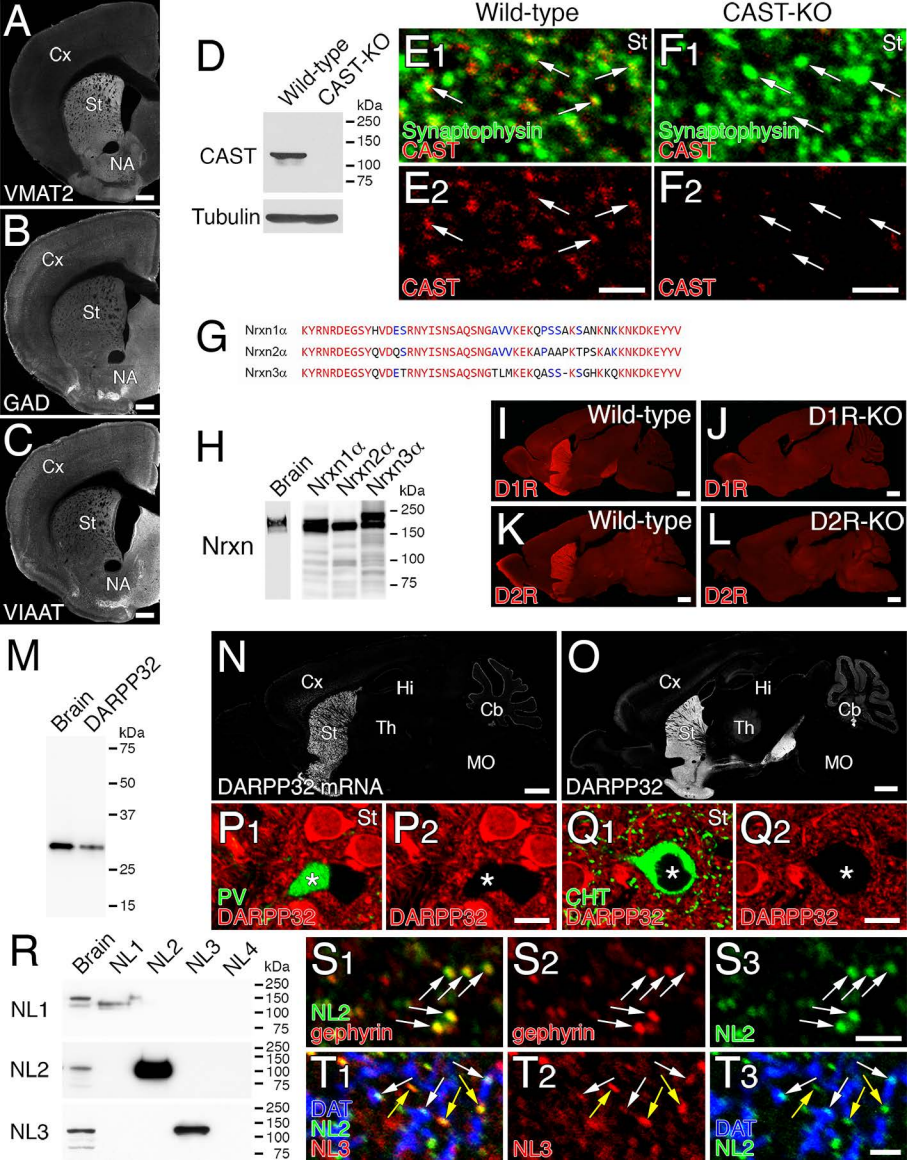
A
Cx
St
NA
VMAT2
B
Cx
St
NA
GAD
C
Cx
St
NA
VIAAT
D
Wild-type
CAST-KO
kDa
250
150
100
75
CAST
Tubulin
Wild-type
CAST-KO
E1
St
Synaptophysin
CAST
F1
St
Synaptophysin
CAST
E2
CAST
F2
CAST
G
Nrxn1α KYRNRDEGSYHVDESRNYISNSAQSNGAVVKEKQPSSAKSANKNKKNKDKEYYV
Nrxn2α KYRNRDEGSYQVDQSRNYISNSAQSNGAVVKEKAPAAPKTPSKAKKNKDKEYYV
Nrxn3α KYRNRDEGSYQVDETRNYISNSAQSNGTLMKEKQASS-KSGHKKQKNKDKEYYV
H
Brain
Nrxn1α
Nrxn2α
Nrxn3α
kDa
250
150
100
75
Nrxn
I
Wild-type
D1R
J
D1R-KO
D1R
K
Wild-type
D2R
L
D2R-KO
D2R
M
Brain
DARPP32
kDa
75
50
37
25
15
N
Cx
Hi
Th
Cb
St
MO
DARPP32 mRNA
O
Cx
Hi
Th
Cb
St
MO
DARPP32
P1
St
PV
DARPP32
P2
DARPP32
Q1
St
CHT
DARPP32
Q2
DARPP32
R
Brain
NL1
NL2
NL3
NL4
kDa
250
150
100
75
NL1
NL2
NL3
S1
NL2
gephyrin
S2
gephyrin
S3
NL2
T1
DAT
NL2
NL3
T2
NL3
T3
DAT
NL2

Table S1

List of primary antibodies used in the present study.

Molecule	Sequence (NCBI #)	Host	Specificity	Reference
$A_{2A}R$	388-410 (NM009630)	GP/Go	IB, KO	(22)
AMPAR	727-745 (X57497)	GP	IB/HEK	(46)
CAST	113-161 (NM_178085)	Rb/GP	IB, KO	this study
CHT	531-580 (BC065089)	Go/GP	IB	(36)
D_1R	402-446 (NM010076)	GP/Go	IB, PT	(22)
D_2R	271–370 (NM010077)	Rb	IB, PT	(22)
DARPP32	163-194 (NM_144828)	Rb/GP	IB/HEK	this study
DAT	1-60 (BC054119)	Rb/GP/Go	IB/HEK	(47)
GABA		Ms		Sigma (A0310) (48)
$GABA_AR\alpha1$	369-386	Rb/GP	IB/HEK	(49)

	(NM_010250)			
GAD65/67	268-593	Go	IB, PT	(48)
	(A28072)			
GAT1	1-46/564-599	Rb/GP	IB/HEK	(49)
	(NM_178703)			
gephyrin	54-94	Rb	IB/HEK	(49)
	(NM_1729529)			
		Ms		Synaptic systems (#147111)
GFP	1-238	Rb/GP/Go	KI	Frontier Institute
	(YP_002302326)			
MAP2	927-1104	Go		(50)
	(NM_008632)			
NL1	46-69	Rb	IB/HEK	this study
	(NM_138666.3)			
NL2	784-829	Rb/GP	IB/HEK	(49)
	(NP_12455)			
NL3	768-793	Rb/GP	IB/HEK	this study
	(NM_172932)			
nNOS	1400-1429	GP	IB	(47)
	(NM_008712)			
Nrxn1α	1454-1507	Rb	IB/HEK, *1	this study,
	(NM_020252)			
PSD-95	1-64	Rb/GP	IB	(51)

	(D50621)			
PV	1-110	Rb/GP/Go		(50)
	(NM_013645)			
synaptophysin		Rb/GP	IB	(51)
TH		Ms/Rb		Immunostar (#22941)
				Millipore (AB152)
VGluT1	531-560aa	Go	IB	(50)
	(BC054462)			
VGluT2	559–582aa	Go	IB	(50)
	(BC038375)			
VGluT3	558-602aa	Go	IB	(52)
	(AF510321)			
VIAAT	31-112	Rb/GP/Go		(50)
	(BC052020)			
VMAT2	468-515	Rb	IB	(52)
	(L00603)			
tau	bovine tau	Ms		Millipore (MAB3420)

$A_{2A}R$, adenosine A_2 receptor; AMPAR, AMPA receptor; CAST, cytomatrix protein at the active zone, also known as ERC2; CHT, high-affinity choline transporter; D_1R/D_2R, dopamine receptor-1/2; DARPP32, dopamine- and cAMP-regulated neuronal phosphoprotein or protein phosphatase 1, regulatory (inhibitory) subunit 1B; DAT, plasmalemmal dopamine transporter; GAD65/67, 65/67-kDa glutamic acid

decarboxylase; GABA, γ-aminobutyric acid; GAT1, plasmalemmal GABA transporter-1; gephyrin, scaffold protein interacting with glycine and $GABA_A$ receptors; GFP, green fluorescent protein; Go, goat polyclonal antibody; GP, guinea pig polyclonal antibody; IB, immunoblot with brain homogenates; IB/HEK, immunoblot with transfected HEK293T cell lysates; KI, specific neuronal labeling in GAD67-GFP knock-in, but not wild-type, mice; KO, no signal in knockout mouse brain; MAP2, microtubule-associated protein-2; Ms, mouse monoclonal antibody; NL1–3, neuroligin-1–3; Nrxn1α, neurexin-1α; nNOS, neuronal nitric oxide synthase; PSD-95, postsynaptic density protein-95; PT, preabsorption test; PV, parvalbumin; TH, tyrosine hydroxylase; VGluT1–3, type 1–3 vesicular glutamate transporter; VIAAT, vesicular inhibitory amino acid transporter; VMAT2, vesicular monoamine transporter-2. *1, Nrxn1α antibody also recognizes Nrxn2α and Nrxn3α owing to high C-terminus homology (Fig. S8H).

Table S2

List of antibodies used for immunohistochemical data.

Figure	1st Antibodies (species)	2nd Antibodies (Company)
1A	TH (Rb)	Cy3 (Jackson Immunoresearch)
1B	DAT (Rb)	Cy3 (Jackson Immunoresearch)
1C	DAT (GP)	A488 (Jackson Immunoresearch)
	VMAT2 (Rb)	Cy3 (Jackson Immunoresearch)
	TH (Mo)	A647 (Life Technologies)
3A	DAT (GP)	A488 (Jackson Immunoresearch)
	$GABA_AR\alpha1$ (Rb)	Cy3 (Jackson Immunoresearch)
	VIAAT (Go)	A647 (Life Technologies)
3B	DAT (GP)	A488 (Jackson Immunoresearch)
	Gephyrin (Mo)	Cy3 (Jackson Immunoresearch)
	VIAAT (Go)	A647 (Life Technologies)
3C	DAT (GP)	A488 (Jackson Immunoresearch)
	NL2 (Rb)	Cy3 (Jackson Immunoresearch)
	VIAAT (Go)	A647 (Life Technologies)
4B	D_1R (GP)	CF405S (Biotium)
	GFP (Go)	A488 (Life Technologies)
	NL2 (Rb)	Cy3 (Jackson Immunoresearch)
	TH (Mo)	A647 (Life Technologies)
4C	$A_{2A}R$ (GP)	CF405S (Biotium)

	GFP (Go)	A488 (Life Technologies)
	NL2 (Rb)	Cy3 (Jackson Immunoresearch)
	TH (Mo)	A647 (Life Technologies)
5B	NL2 (Rb)	A488 (Life Technologies)
	DAT (Go)	Cy3 (Jackson Immunoresearch)
	CAST (GP)	A647 (Jackson Immunoresearch)
5C	$GABA_AR\alpha1$ (Rb)	A488 (Life Technologies)
	DAT (Go)	Cy3 (Jackson Immunoresearch)
	CAST (GP)	A647 (Jackson Immunoresearch)
5D	GFP (Rb)	A488 (Life Technologies)
	DAT (Go)	Cy3 (Jackson Immunoresearch)
	CAST (GP)	A647 (Jackson Immunoresearch)
5F	NL2 (GP)	A488 (Jackson Immunoresearch)
	DAT (Go)	Cy3 (Jackson Immunoresearch)
	VMAT2 (Rb)	A647 (Life Technologies)
5G	NL2 (GP)	A488 (Jackson Immunoresearch)
	DAT (Go)	Cy3 (Jackson Immunoresearch)
	Nrxn (Rb)	A647 (Life Technologies)
6A–6C	VIAAT (Go)	A405 (Abcam)
	GFP (GP)	A488 (Jackson Immunoresearch)
	TH (Rb)	Cy3 (Jackson Immunoresearch)
	Gephyrin (Mo)	A647 (Life Technologies)
S1A	DAT (Go)	A488 (Life Technologies)

	VGluT1 (Rb)	Cy3 (Jackson Immunoresearch)
S1B	DAT (Go)	A488 (Life Technologies)
	VGluT2 (GP)	Cy3 (Jackson Immunoresearch)
S1C	DAT (Go)	A488 (Life Technologies)
	VGluT3 (GP)	Cy3 (Jackson Immunoresearch)
S1D	DAT (Go)	A488 (Life Technologies)
	GAD (Rb)	Cy3 (Jackson Immunoresearch)
S1E	DAT (Go)	A488 (Life Technologies)
	VIAAT (Rb)	Cy3 (Jackson Immunoresearch)
S1F	DAT (Go)	A488 (Life Technologies)
	GAT1 (Rb)	Cy3 (Jackson Immunoresearch)
S1G	DAT (Go)	A488 (Life Technologies)
	GAT1 (Rb)	Cy3 (Jackson Immunoresearch)
	VIAAT (GP)	A647 (Jackson Immunoresearch)
S1H	DAT (Go)	A488 (Life Technologies)
	CAST (GP)	Cy3 (Jackson Immunoresearch)
S2B	D_1R (GP)	A488 (Jackson Immunoresearch)
	D_2R (Rb)	Cy3 (Jackson Immunoresearch)
S2C	MAP2 (Mo)	A405 (Abcam)
	DARPP32 (GP)	A488 (Jackson Immunoresearch)
	D_2R (Rb)	Cy3 (Jackson Immunoresearch)
	D_1R (Go)	A647 (Life Technologies)
S2D	MAP2 (Mo)	A405 (Abcam)

	PV (GP)	A488 (Jackson Immunoresearch)
	D_2R (Rb)	Cy3 (Jackson Immunoresearch)
	D_1R (Go)	A647 (Life Technologies)
S2E	MAP2 (Mo)	A405 (Abcam)
	nNOS (GP)	A488 (Jackson Immunoresearch)
	D_2R (Rb)	Cy3 (Jackson Immunoresearch)
	D_1R (Go)	A647 (Life Technologies)
S2F	MAP2 (Mo)	A405 (Abcam)
	CHT (GP)	A488 (Jackson Immunoresearch)
	D_2R (Rb)	Cy3 (Jackson Immunoresearch)
	D_1R (Go)	A647 (Life Technologies)
S2G	Tau (Mo)	A488 (Life Technologies)
	D_1R (GP)	Cy3 (Jackson Immunoresearch)
	DARPP32 (Rb)	A647 (Life Technologies)
S2H	Tau (Mo)	A488 (Life Technologies)
	D_2R (Rb)	Cy3 (Jackson Immunoresearch)
	CHT (GP)	A647 (Jackson Immunoresearch)
S2I	Tau (Mo)	A488 (Life Technologies)
	D_2R (Rb)	Cy3 (Jackson Immunoresearch)
	DAT (Go)	A647 (Life Technologies)
S4A, S4B	GFP (Rb)	A488 (Life Technologies)
S4C	PV (GP)	CF405S (Biotium)
	GFP (Go)	A488 (Life Technologies)

	NL2 (Rb)	Cy3 (Jackson Immunoresearch)
	TH (Mo)	A647 (Life Technologies)
S4D	nNOS (GP)	CF405S (Biotium)
	GFP (Go)	A488 (Life Technologies)
	NL2 (Rb)	Cy3 (Jackson Immunoresearch)
	TH (Mo)	A647 (Life Technologies)
S4E	CHT (GP)	CF405S (Biotium)
	GFP (Go)	A488 (Life Technologies)
	NL2 (Rb)	Cy3 (Jackson Immunoresearch)
	TH (Mo)	A647 (Life Technologies)
S5B	NL2 (Rb)	A488 (Life Technologies)
	Tau (Mo)	Cy3 (Jackson Immunoresearch)
	CAST (GP)	A647 (Jackson Immunoresearch)
S5C	$GABA_AR\alpha1$ (Rb)	A488 (Life Technologies)
	Tau (Mo)	Cy3 (Jackson Immunoresearch)
	CAST (GP)	A647 (Jackson Immunoresearch)
S5D	GFP (Rb)	A488 (Life Technologies)
	Tau (Mo)	Cy3 (Jackson Immunoresearch)
	CAST (GP)	A647 (Jackson Immunoresearch)
S5F	NL3 (Rb)	A488 (Life Technologies)
	Tau (Mo)	Cy3 (Jackson Immunoresearch)
	CAST (GP)	A647 (Jackson Immunoresearch)
S6H, S6I	VMAT2 (Rb)	Cy3 (Jackson Immunoresearch)

S6M, S6N	Gephyrin (Mo)	Cy3 (Jackson Immunoresearch)
S6R, S6S	NL3 (GP)	Cy3 (Jackson Immunoresearch)
S7C	GFP (Rb)	A488 (Life Technologies)
	DARPP32 (GP)	Cy3 (Jackson Immunoresearch)
S7D–S7F	GFP (Go)	A488 (Life Technologies)
	Gephyrin (Mo)	Cy3 (Jackson Immunoresearch)
	NL2 (Rb)	A647 (Life Technologies)
S7J–S7L	GFP (Go)	A488 (Life Technologies)
	Gephyrin (Mo)	Cy3 (Jackson Immunoresearch)
	NL3 (GP)	A647 (Jackson Immunoresearch)
S8A	VMAT2 (Rb)	Cy3 (Jackson Immunoresearch)
S8B	GAD (Rb)	Cy3 (Jackson Immunoresearch)
S8C	VIAAT (Rb)	Cy3 (Jackson Immunoresearch)
S8E–S8F	Synaptophysin (Rb)	A488 (Life Technologies)
	CAST (GP)	Cy3 (Jackson Immunoresearch)
S8I, S8J	D_1R (GP or Go)	Cy3 (Jackson Immunoresearch)
S8K, S8L	D_2R (Rb)	Cy3 (Jackson Immunoresearch)
S8O	DARPP32 (GP or Rb)	Cy3 (Jackson Immunoresearch)
S8P	PV (Rb)	A488 (Life Technologies)
	DARPP32 (GP)	Cy3 (Jackson Immunoresearch)
S8Q	CHT (Rb)	A488 (Life Technologies)
	DARPP32 (GP)	Cy3 (Jackson Immunoresearch)

S8S	NL2 (Rb)	A488 (Life Technologies)
	Gephyrin (Mo)	Cy3 (Jackson Immunoresearch)
S8T	NL2 (Rb)	A488 (Life Technologies)
	NL3 (GP)	Cy3 (Jackson Immunoresearch)
	DAT (Go)	A647 (Life Technologies)

Go, goat; GP, guinea pig; Mo, mouse; Rb, rabbit; A405, Alexa405; A488, Alexa488; A647, Alexa647

Table S3

The labeling density of synaptic molecules in individual mice.

Mouse	Synapse type	Molecule	Synapse #	Labeling density (mean ± SEM)	Figure
WT #1	DA	GABA	9	61.7 ± 11.6	1F
WT #2	DA	GABA	5	38.2 ± 8.20	1F
WT #3	DA	GABA	6	19.4 ± 3.24	1F
WT #1	GABA	GABA	9	594 ± 109	1F
WT #2	GABA	GABA	5	336 ± 68.8	1F
WT #3	GABA	GABA	6	284 ± 40.8	1F
WT #1	Glu	GABA	11	40.7 ± 22.9	1F
WT #2	Glu	GABA	9	16.5 ± 7.01	1F
WT #3	Glu	GABA	5	8.03 ± 3.51	1F
WT #4	DA	CAST	15	4.26 ± 2.19	1H
WT #5	DA	CAST	15	4.38 ± 0.776	1H
WT #6	DA	CAST	13	1.76 ± 0.776	1H
CAST-KO #1	DA	CAST	10	0 ± 0	1H
CAST-KO #2	DA	CAST	11	0.57 ± 0.57	1H
CAST-KO #3	DA	CAST	14	0 ± 0	1H
WT #4	GABA	CAST	9	1.28 ± 0.86	1H
WT #5	GABA	CAST	9	1.15 ± 0.82	1H
WT #6	GABA	CAST	10	2.45 ± 1.39	1H

24	CAST-KO #1	GABA	CAST	12	0 ± 0	1H
25	CAST-KO #2	GABA	CAST	12	0.49 ± 0.49	1H
26	CAST-KO #3	GABA	CAST	8	0 ± 0	1H
27	WT #4	Glu	CAST	11	40.7 ± 22.9	1H
28	WT #5	Glu	CAST	8	16.5 ± 7.01	1H
29	WT #6	Glu	CAST	5	8.03 ± 3.51	1H
30	CAST-KO #1	Glu	CAST	5	0 ± 0	1H
31	CAST-KO #2	Glu	CAST	9	0 ± 0	1H
32	CAST-KO #3	Glu	CAST	8	0 ± 0	1H
33	WT #7	DA	Nrxn	5	7.75 ± 3.87	1J
34	WT #8	DA	Nrxn	7	1.94 ± 1.26	1J
35	WT #9	DA	Nrxn	10	3.54 ± 1.84	1J
36	WT #7	GABA	Nrxn	8	5.34 ± 3.91	1J
37	WT #8	GABA	Nrxn	7	2.92 ± 1.39	1J
38	WT #9	GABA	Nrxn	10	1.92 ± 0.866	1J
39	WT #7	Glu	Nrxn	6	4.91 ± 1.63	1J
40	WT #8	Glu	Nrxn	8	2.90 ± 1.15	1J
41	WT #9	Glu	Nrxn	7	3.84 ± 1.91	1J
42	WT #7	DA	$GABA_AR\alpha1$	12	8.87 ± 4.00	3G
43	WT #8	DA	$GABA_AR\alpha1$	10	11.1 ± 4.19	3G
44	WT #9	DA	$GABA_AR\alpha1$	10	4.47 ± 2.53	3G
45	WT #7	GABA	$GABA_AR\alpha1$	11	6.59 ± 1.97	3G
46	WT #8	GABA	$GABA_AR\alpha1$	13	7.54 ±1.81	3G

47	WT #9	GABA	$GABA_AR\alpha1$	12	6.69 ± 1.83	3G
48	WT #7	Glu	$GABA_AR\alpha1$	7	0 ± 0	3G
49	WT #8	Glu	$GABA_AR\alpha1$	7	0 ± 0	3G
50	WT #9	Glu	$GABA_AR\alpha1$	11	0.197 ± 0.197	3G
51	WT #7	DA	Gephyrin	10	31.7 ± 8.19	3H, S5S
52	WT #8	DA	Gephyrin	7	25.5 ± 8.22	3H, S5S
53	WT #9	DA	Gephyrin	8	27.9 ± 4.20	3H, S5S
54	NL2-KO #1	DA	Gephyrin	5	28.3 ± 11.1	S5S
55	NL2-KO #2	DA	Gephyrin	5	45.8 ± 16.0	S5S
56	NL2-KO #3	DA	Gephyrin	5	10.0 ± 2.98	S5S
57	WT #7	GABA	Gephyrin	11	29.7 ± 6.02	3H
58	WT #8	GABA	Gephyrin	12	15.9 ± 4.36	3H
59	WT #9	GABA	Gephyrin	10	22.0 ± 5.95	3H
60	WT #7	Glu	Gephyrin	5	0 ± 0	3H
61	WT #8	Glu	Gephyrin	6	0.48 ± 0.48	3H
62	WT #9	Glu	Gephyrin	10	0 ± 0	3H
63	WT #7	DA	NL2	11	12.0 ± 4.60	3I
64	WT #8	DA	NL2	6	12.0 ± 4.30	3I
65	WT #9	DA	NL2	9	13.5 ± 4.07	3I
66	NL2-KO #1	DA	NL2	5	0 ± 0	3I
67	NL2-KO #2	DA	NL2	7	0 ± 0	3I
68	NL2-KO #3	DA	NL2	6	0.991 ± 0.991	3I
69	WT #7	GABA	NL2	7	10.8 ± 4.49	3I

70	WT #8	GABA	NL2	12	8.39 ± 1.99	3I
71	WT #9	GABA	NL2	10	10.5 ± 2.32	3I
72	WT #7	Glu	NL2	8	0.68 ± 0.54	3I
73	WT #8	Glu	NL2	6	0 ± 0	3I
74	WT #9	Glu	NL2	7	0.326 ± 0.326	3I
75	WT #7	DA	PSD-95	8	0 ± 0	S3F
76	WT #8	DA	PSD-95	6	0 ± 0	S3F
77	WT #9	DA	PSD-95	7	0 ± 0	S3F
78	WT #7	GABA	PSD-95	5	0 ± 0	S3F
79	WT #8	GABA	PSD-95	9	0 ± 0	S3F
80	WT #9	GABA	PSD-95	10	0 ± 0	S3F
81	WT #7	Glu	PSD-95	5	25.6 ± 6.15	S3F
82	WT #8	Glu	PSD-95	5	19.0 ± 7.12	S3F
83	WT #9	Glu	PSD-95	9	40.8 ± 5.65	S3F
84	WT #7	DA	AMPAR	6	0 ± 0	S3G
85	WT #8	DA	AMPAR	9	0 ± 0	S3G
86	WT #9	DA	AMPAR	6	0 ± 0	S3G
87	WT #7	GABA	AMPAR	6	0 ± 0	S3G
88	WT #8	GABA	AMPAR	11	0.939 ± 0.939	S3G
89	WT #9	GABA	AMPAR	11	0 ± 0	S3G
90	WT #7	Glu	AMPAR	6	13.7 ± 3.34	S3G
91	WT #8	Glu	AMPAR	5	16.4 ± 5.95	S3G
92	WT #9	Glu	AMPAR	5	18.7 ± 7.79	S3G

93	WT #10	DA	VMAT2	7	78.9 ± 8.30	S5N
94	WT #11	DA	VMAT2	6	86.9 ± 13.2	S5N
95	WT #12	DA	VMAT2	6	74.2 ± 16.5	S5N
96	NL2-KO #4	DA	VMAT2	7	83.7 ± 15.3	S5N
97	NL2-KO #5	DA	VMAT2	7	66.8 ± 5.75	S5N
98	NL2-KO #6	DA	VMAT2	6	93.5 ± 16.2	S5N
99	WT #7	DA	NL3	8	1.06 ± 1.06	S5X
100	WT #8	DA	NL3	6	3.17 ± 2.02	S5X
101	WT #9	DA	NL3	5	1.85 ± 1.85	S5X
102	NL2-KO #1	DA	NL3	6	9.03 ± 4.37	S5X
103	NL2-KO #2	DA	NL3	6	12.2 ± 10.7	S5X
104	NL2-KO #3	DA	NL3	5	15.2 ± 4.16	S5X

105 _____

106 WT, wild-type mouse; DA dopamine synapse; GABA, GABAergic synapse, Glu,
107 glutamatergic synapses. The density for GABA and VMAT2 is represented as the number
108 of metal particles per 1 μm^2 of the terminal. The density for other molecules is represented
109 as the number of metal particles per 1 μm of the presynaptic or postsynaptic membrane.